

## Optimization of Waterjet Propelled High Speed Ships - JHSS and Delft Catamaran

Manivanman Kandasamy<sup>1</sup>, Wei He<sup>1</sup>, Tomohiro Takai<sup>1</sup>, Yusuke Tahara<sup>2</sup>, Daniele Peri<sup>3</sup>, Emilio Campana<sup>3</sup>, Wesley Wilson<sup>4</sup>, and Frederick Stern<sup>1</sup>

<sup>1</sup> IIHR-Hydroscience & Engineering, the University of Iowa

<sup>2</sup> NMRI-National Maritime Research Institute, Japan

<sup>3</sup> INSEAN- Italian Ship Model basin

<sup>4</sup> DTMB - David Taylor Model Basin

### ABSTRACT

The present work focuses on the application of Simulation Based Design (SBD) for the resistance optimization of two waterjet propelled high-speed ships, namely, the Joint High Speed Sea-lift (JHSS) which is a monohull, and the Delft Catamaran (DC) at  $Fr=0.34$  and 0.5, respectively. Design optimization has been performed for both the parent hull form and the waterjet inlets. The adopted SBD explores the concept of variable physics approach for the Delft catamaran which shows strong waterjet hull interaction effects. First a simplified CFD waterjet model is used to include the waterjet induced forces and moments during the bare hull Delft catamaran optimization. Next, the waterjet is appended to the optimized barehull and the inlet is optimized by detailed simulation of the duct flow. The bow shape optimization and waterjet inlet optimization of the JHSS were done independent of each other since waterjet hull interactions are weak, and the bow shape modification does not affect the local flow near the waterjet inlet. For JHSS, which has four side by side axial waterjets, the effect of combining the waterjet inlets on the powering performance was also explored. The design optimization yielded geometries with significant resistance reduction for both the JHSS and Delft catamaran. The final optimized Delft catamaran will be built and model tested to validate the SBD process.

### KEY WORDS

Particle Swarm Optimization, Delft catamaran, JHSS, Water-jet propelled high-speed ships, Variable Physics, Waterjet model

### 1.0 INTRODUCTION

Nowadays, there is a growing interest in waterjet propulsion because it has a lot of benefits over conventional screw propeller such as shallow draft design, smooth engine load, less vibration, lower water borne noise, no appendage drag, better efficiency at high speeds and good maneuverability. Pre-designed waterjets are readily available to be outfitted to any type of vessel based on the engine power, resistance curves, and the design speed of the ship. However, the performance of the waterjet systems, with respect to inlet

efficiency, velocity distribution at the impeller plane, and cavitation inception at cutwater are determined by the inlet velocity ratio, which depends on the specific hull shape and speed of operation. To get best performance of the waterjet propulsion system, the above factors should be taken into account for optimization of the pre-designed waterjet inlet.

In the current paper design optimization is carried out for both the hull form and the waterjet inlet, with resistance/powering performance as the single objective function for both JHSS (at  $Fr=0.34$ ) and Delft catamaran (at  $Fr=0.5$ ). For the waterjet inlet design, this implies the optimization of the inlet efficiency. Cavitation and non-uniformity of velocity distribution at the inlet plane are not considered in the current study. Since viscous effects involving boundary layer ingestion play an significant part in the waterjet inlet performance, variable fidelity approaches which integrate potential flow methods with URANS through metamodels cannot be used reliably for waterjet inlet design optimization. However, the variable fidelity approach can be used for optimization of the barehull with the incorporation of waterjet induced forces and moments through a variable physics approach by using the integral force/moment CFD waterjet model (Kandasamy *et al.*, 2010). Tahara *et al.* (2011) use this variable fidelity/physics approach in a concurrent and complementary paper for the multi objective design optimization of resistance and sea-keeping of the barehull JHSS and Delft catamaran without discretization of the waterjet duct flow. The current study employs just the variable physics method for Delft catamaran, where the initial optimization of the bare hull is conducted with the waterjet model and the selected optimized barehull is appended with the waterjet and the waterjet inlet is optimized.

As a pre-requisite to the optimization, the method used here for the waterjet simulation has been validated with experimental data for both JHSS (Takai *et al.*, 2011) and the Delft catamaran (Kandasamy *et al.*, 2011). The approach uses URANS with a single phase level set method for the free-surface prediction, with an actuator disk model to replicate the effects of the impeller, and two degrees of motion were allowed for dynamic sinkage and trim predictions.

The Simulation Based Design (SBD) toolkit used here is a product of the long-term collaboration between IIHR, INSEAN and NMRI research groups. The SBD toolbox provides high fidelity/low fidelity flow solvers, multiple optimization algorithms, and different geometry/grid modification methods (Campana *et al.*, 2009). Previous versions of the tool box have been successfully used in the optimization of high speed monohull (Campana *et al.*, 2006, Tahara *et al.*, 2008a) and multihull (Tahara *et al.*, 2008b, Peri *et al.*, 2010) displacement ships and foil-assisted semi-planing catamaran ferries (Kandasamy *et al.*, 2009). This is the first time the toolkit is being used for waterjet propelled ships.

The remainder of the paper will be structured as follows: section 2 gives an overview of the SBD methodology with brief description of the optimizer, geometry modification technique and the solver used for the current study; section 3 gives details of the sensitivity studies conducted on the JHSS and Delft catamaran hulls and waterjet inlets prior to the optimization, in order to select a feasible design space to investigate; section 4 provides the results from the optimization, and section 5 provides the conclusions from the current study and directions for future work.

## 2.0 SBD methodology

The SBD methodology comprises of three main parts: the optimizer, the geometry modification methods and the flow solver. The flow solver sends the evaluated objective function for a certain set of design variables to an optimizer, which searches for the minimum value under the general mathematical framework of a Non-Linear Programming problem and continually updates the design variables. Geometry modeling methods provides the link between the two by deforming the hull shape based on the updated design variables.

### 2.1 Optimizer

The particle swarm optimizer (PSO) was chosen for the current design optimization because recent studies (Takai, 2010) using analytical function based search space indicated that it converges faster to the global minimum for single objective optimization problems compared to evolutionary global optimization methods. The PSO strategy simulates the social behavior of a set of particles which share information among them while exploring the design variables' space. In the basic PSO method, each particle has its own memory (parameter 1) to remember the best places that it has visited, whereas the swarm has a global memory (parameter 2) to remember the best place ever visited. Parameters 1 and 2 are called the cognitive and social parameters, respectively. The cognitive parameter indicates how much confidence the particle has in itself, while the social parameter indicates how much confidence it has in the swarm. A random parameter (parameter 3) is applied to the cognitive and social parameters. Each particle has an adaptable velocity based on these parameters to move itself across the design space. According to these principles, each

particle investigates the search space analyzing its own travel experience and that of the other members of the swarm. Inertia weights (parameter 4) controls the impact of the previous velocities on the current velocity and hence regulates the trade-off between global (wide ranging) and local (nearby) exploration of the swarm. Fine tuning of these parameters is crucial for the optimization process, and the final solution and the calculation time are strictly linked to the parameters setting. (Campana *et al.*, 2009)

### 2.2 Geometry modification methods

There exist a large number of approaches for geometry modification: simple morphing techniques, B-spline control point modifications, CAD systems, and Free Form Deformation (FFD) techniques. The morphing method was chosen for the current optimization due to the ease of transition from the sensitivity studies to optimization. The best geometries obtained from the sensitivity studies are simply transitioned to the optimizer. The design space is thus directly defined by the initial geometries which will be blended with weighting coefficients during optimization. The number of design variables required is one less than the number of geometries used for the morphing, *e.g.*, two design variables are used for three-hull-form blending as shown in Eq. [1].

$$\mathbf{P}_{new} = w_1 \mathbf{P}_1 + w_2 \mathbf{P}_2 + w_3 \mathbf{P}_3$$

where [1]

$$\begin{aligned} w_1 &= x_1 \\ w_2 &= (1-x_1)x_2 \\ w_3 &= (1-x_1)(1-x_2) \end{aligned}$$

so that  $w_1 + w_2 + w_3 = 1$

$\mathbf{P}_{new}$  denotes the grid points of the morphed grid,  $\mathbf{P}_{1-3}$  are the grid points for the three initial designs with  $w_{1-3}$  as the corresponding weighting coefficients.  $x_1$  and  $x_2$  are the design variables that determine  $w_{1-3}$ .

The initial geometries for the sensitivity studies can be generated using any technique: FFD, B-spline modification, or direct modification of the grid in a grid generation software. The only stipulation is that all the initial grids need to have the same topology and grid size.

Another benefit of the morphing method is that the geometric constraints are automatically satisfied during optimization, as long as the initial designs satisfy the geometric constraints.

### 2.3 Flow Solver

The URANS solver, CFDSHIP-IOWA (Carrica *et al.*, 2010) is used with the blended k- $\epsilon$ /k- $\omega$  turbulent and a single phase level set method to predict the free surface. A second order upwind scheme is used to discretize the convective terms of momentum equations for URANS. A pressure-implicit split-operator (PISO) algorithm is used to enforce mass conservation on the collocated grids. The pressure Poisson equation is solved using the PETSc toolkit. All the other systems are solved using an alternating direction implicit (ADI) method. For a high performance parallel

computing, a MPI-based domain decomposition approach is used, where each decomposed block is mapped to one processor. The code SUGGAR runs as a separate process from the flow solver to compute interpolation coefficients for the overset grids and communicates with a motion controller (6DOF) within CFDShip at every timestep. The software USURP is used to compute area and forces on the surface overlapped regions. In addition, a simplified body force model is used for waterjet propelled simulation to prescribe axisymmetric body force with axial and tangential components. The propeller model requires thrust, torque, and advance coefficients as input and provides the torque and thrust forces. These forces appear as a body force term in the momentum equations for the fluid inside the propeller disk. The location of the propeller is defined in the static condition of the ship and moves according to the ship motions.

The waterjet appended JHSS is shown in Fig. 1. The geometry has four waterjet ducts side by side, and a half domain grid utilized 15 overset blocks for the two waterjet ducts.

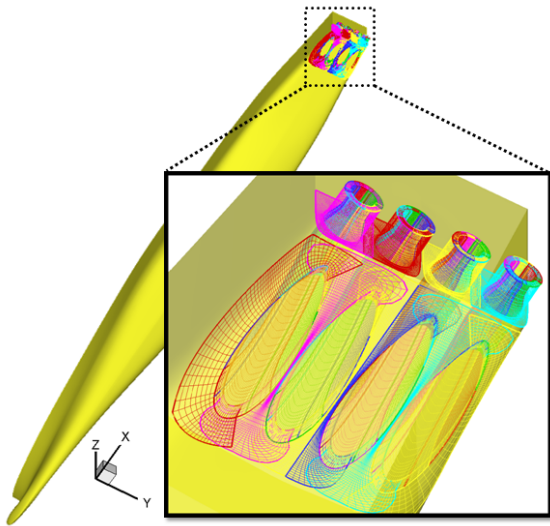


**Fig. 1.** Waterjet appended JHSS geometry

Evaluation of the results during the validation phase showed that the extensive use of overset grids inside the duct leads to a defect in mass conservation due to interpolation errors (Takai *et al.*, 2011). An accurate flow rate measurement is important since the estimation of power is dependent upon velocity cubed, and thrust by the velocity squared. Based on this observation, the Delft catamaran waterjet duct was discretized using a single structured grid, which overlaps with the hull grid at the inlet and the nozzle exit (Fig. 2). A symmetry boundary condition was used, and body-fitted “O” type grids are generated around the port side ship hull geometry. A rectangular background grid is used with clustered grid near the free surface to resolve the wave field. A cylindrical refinement block was generated immediately following the nozzle exit to better resolve the exiting jet.

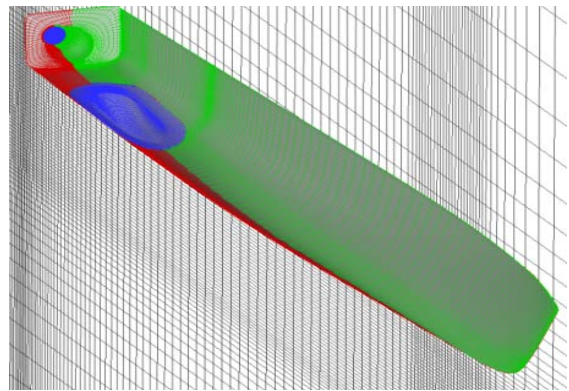


**Fig. 2.** Overset grid system for DC

Details of the solution domain, grid, and boundary conditions for the JHSS and Delft catamaran can be found in Takai *et al.* (2011) and Kandasamy *et al.* (2011), respectively. Fig. 3a & 3b show the volume flow solutions got for the original waterjet appended JHSS and the Delft catamaran. Note that for the Delft catamaran, the waterjet inflow is greatly dependent on the hull contour, whereas the JHSS has a flat bottom and a straightforward inlet capture area. Hence, for the delft catamaran, it is imperative that the design optimization of the hull form and the waterjet inlet be coupled.

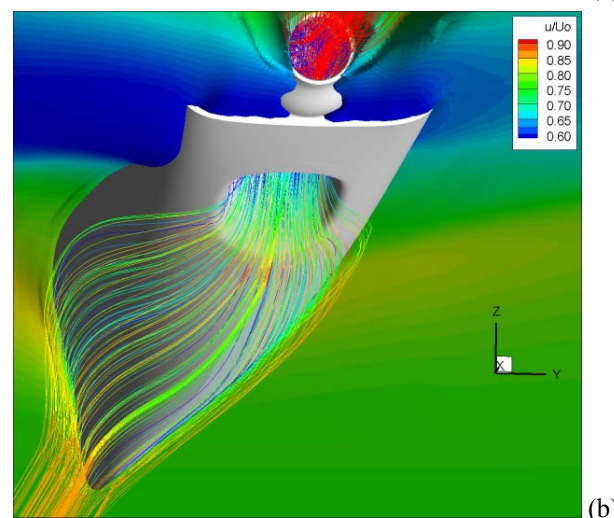
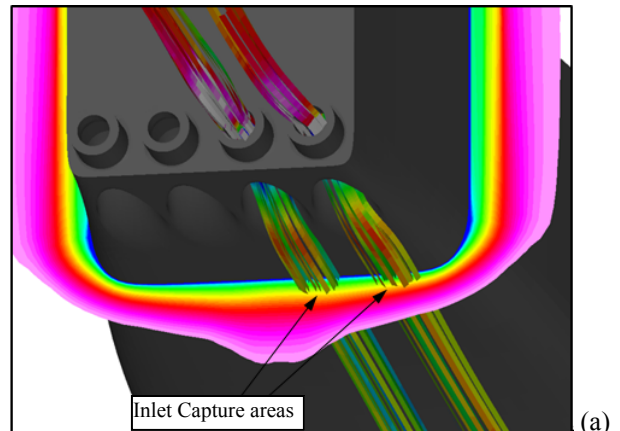


**Fig. 3.** Volume flow solutions: (a) JHSS at  $Fr=0.34$ , (b) DC at  $Fr=0.53$ .

### 3.0 Initial sensitivity studies to generate base geometries for blending

Initial sensitivity studies were conducted on the hull and waterjet inlet to determine a feasible design space.

#### 3.1 JHSS bow sensitivity

For JHSS, the shape sensitivity studies focussed only on the gooseneck bow, and the hull was left unaltered. The sensitivity studies explored the effect of altering the bow width and the depth (Fig. 4) using B-splines.

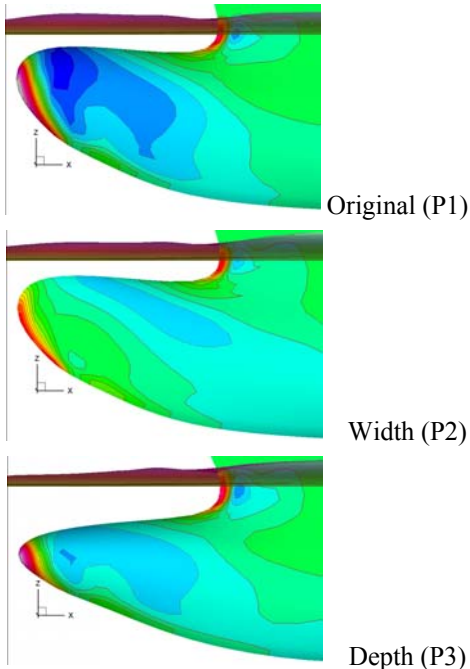


**Fig. 4.** Bow shape sensitivity studies for JHSS, selected designs for morphing

The best design from reduction of the bow width (P2) gave a 6.7% reduction, and the best design from variation of the bow depth (P3) gave a 3.5% reduction in resistance. The original geometry (P1), P2 and P3 constitute the initial designs defining the search space with two design variables.

#### 3.2 JHSS waterjet inlet sensitivity

Two types of geometry modification were performed for the JHSS waterjet inlet, one on the upper duct Gaussian curvature and one on the cut water region, both using B-splines (Fig. 5). The best designs (Fig. 6) from both types of geometry modification showed ~1% decrease in total resistance (pressure and friction resistance integrated over both the hull and the waterjet interior surface).

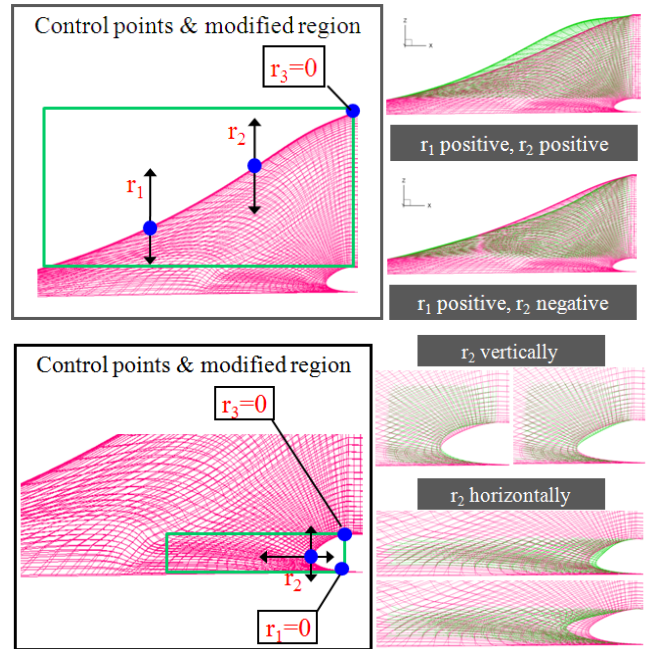


**Fig. 5.** Inlet shape sensitivity studies for JHSS

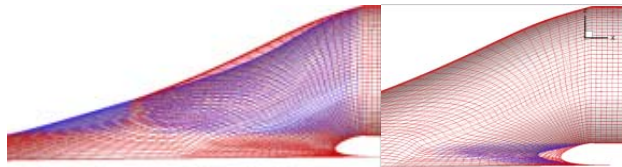


**Fig. 6.** Selected JHSS waterjet designs for morphing

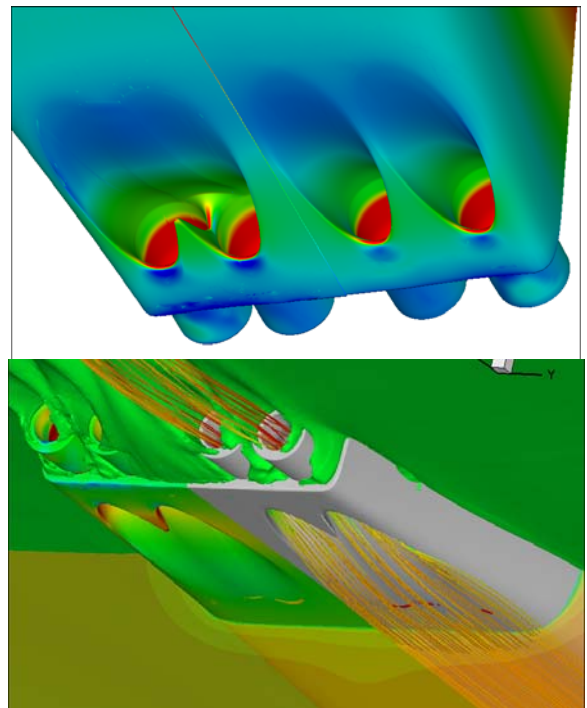


**Fig. 7.** Merged Inlets for JHSS

A completely different approach of combining the waterjet inlets in order to decrease the overall surface area of the inlets was investigated (Fig. 7). Not only is the surface area reduced, the inlet capture area are combined allowing for more boundary layer ingestion. Results showed ~7% decrease in total resistance. However, there other issues to be considered such as structural integrity and effect of cross flow during manoeuvring before a combined inlet design can be deemed feasible.

### 3.3 DC hull shape sensitivity

For the Delft catamaran, six different hull shapes, including the original were selected for morphing (Fig. 8). DC1, DC2 and DC3 were created using B-spline modification of the original hull shape. DC1 was created by asymmetric deformation of the bow. DC2 and DC3 were created by increasing the slenderness ratio of the demi-hulls within limits imposed by the diameter of the waterjet impeller. DC4 and DC5 were created by asymmetric free form deformation of the hulls. The modified geometries showed ~1-2% reduction in resistance compared to the original.

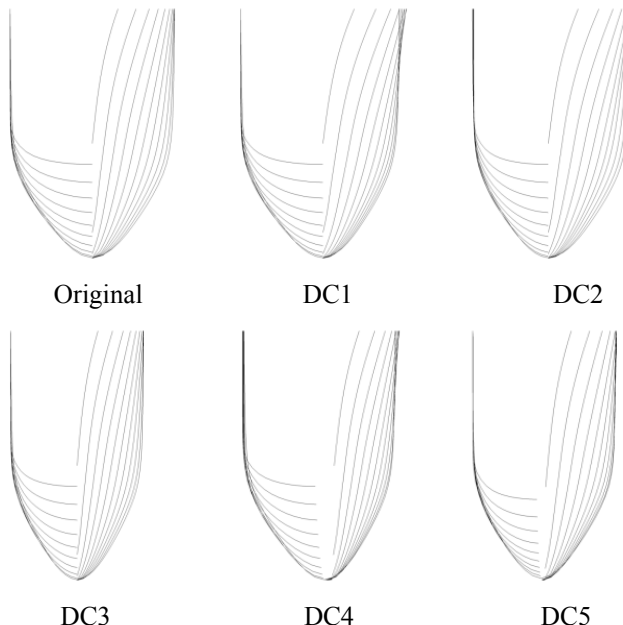


**Fig. 8.** Initial demihull selections for DC bare-hull optimization for morphing

### 3.4 DC waterjet inlet sensitivity

Similar to the JHSS inlet sensitivity studies, two types of geometry modification were performed for the DC waterjet inlet, one on the upper duct Gaussian curvature, and one on the cut water region, both using B-splines (Fig. 9).



**Fig. 9.** Selected initial DC waterjet duct geometries for morphing

The modification of the upper curvature provided a geometry with ~2% reduction in total resistance and the cut water modification provided a geometry with ~1% reduction in total resistance.

## 4.0 OPTIMIZATION

### 4.1 JHSS barehull optimization

The optimization problem is defined in Table 1. The optimization was carried out for a single objective function, *i.e.*, minimize resistance at  $Fr=0.34$ , with constraints on the length, beam and displacement. During sensitivity studies, the solver experienced divergence for extreme deformations of the bow, and hence the design variables were constrained within limits  $0 < x_1, x_2 < 1$ . However, even with the constraints on the design variables, the PSO initially allows the particles to go out of bounds, and then the particles implode to explore the entire bounded region.

**Table 1.** Optimization problem for JHSS bow

Objective function	Geometrical Constraints	Design var. constraints
Minimize: $F1 = R_f$ Target speed: $Fr=0.34$ Sea condition: calm	Waterline length $Lwl$ , Maximum beam $B_{(max)}$ & Draft $T = \text{constant}$ Displacement $\Delta = \text{constant}$	$0 < x_1, x_2 < 1$

Testing of the PSO on analytical functions with two design variables showed that 4 particles were sufficient to find the global minimum. Based on this, two separate optimization simulations were conducted for the JHSS bow form, first with 4, and next with 6 particles. The topological map of the objective function in the explored region of the search space, obtained by interpolating the particle objective function values, is shown in Fig. 10.

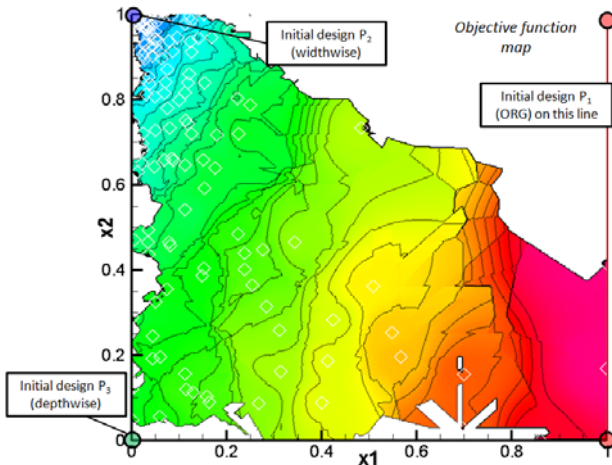


**Fig. 10.** Topology map of objective function for the JHSS bow shape design space.

The particles converge at  $(x_1, x_2)=(0, 1)$ , indicating the best design within the search space is the initial design P2. Both PSO approaches, *i.e.*, with 4 and 6 particles converge at the same location after 30 iteration as seen in Fig. 11. The total number of simulations for the 4 particle and 6 particles cases are 120 and 180, respectively.

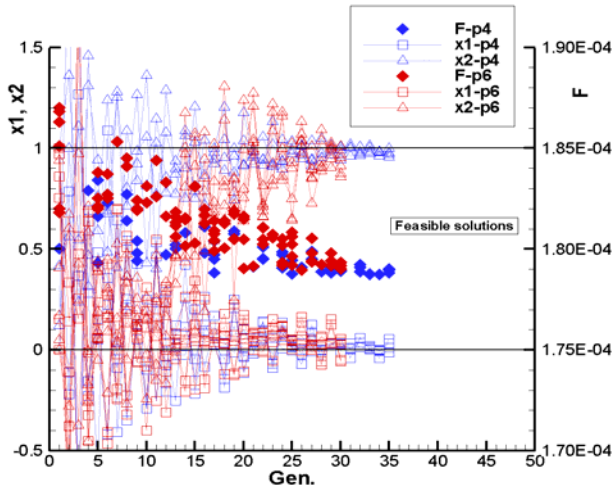


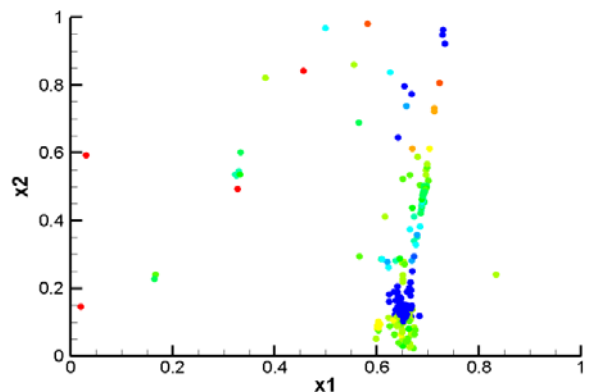
**Fig. 11.** Convergence of the design variables and the objective function for JHSS bow form optimization.

Tahara *et al.* (2011) conducted the concurrent and complimentary multi-objective genetic algorithm optimization for resistance and sea-keeping using the same initial geometries, with the same morphing approach and the same solver, thus exploring the same design space. They found the minimal value at  $(x_1, x_2)=(0.35, 1)$  after evaluating 400 points in the map. This lies in the unexplored region of the PSO topology map indicating that the particles got stuck at a local minima during PSO optimization.

## 4.2 JHSS waterjet inlet optimization

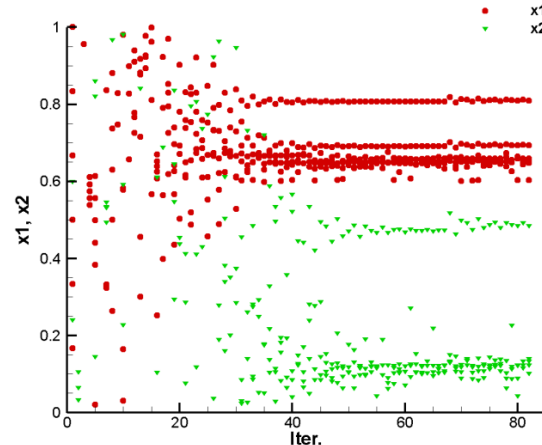
For the JHSS waterjet inlet, the optimization problem is the same as for the barehull optimization. The optimization was carried out with the waterjet appended on the original JHSS hull form since the bow form modification does not alter the local flow near the waterjet inlet.

A six particle swarm approach was used here. The design space is sparingly explored before the particles converge (Fig. 12) and hence reliable interpolation is not possible to get a topology map similar to the one shown for the bare hull optimization. The topology map for the bare hull is better defined only because the map was generated using particles from the two different optimization studies with different particle trajectories.



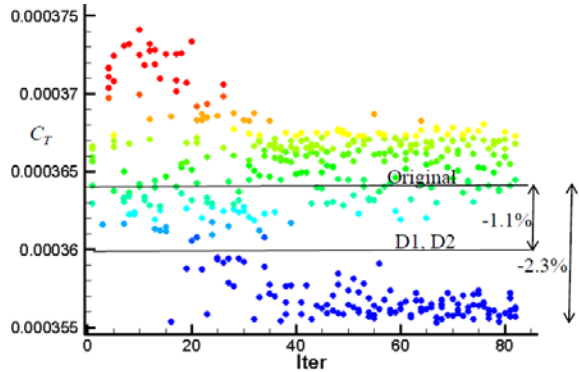
**Fig. 12.** Topology map of the objective functions for JHSS waterjet inlet design space, particles colored with objective function

Fig. 13 shows the convergence of the particles with the minimum search value occurring at  $(x_1, x_2)=(0.65, 0.1)$ . A few particles get stuck at other local minima.



**Fig. 13.** Convergence of design variables for JHSS waterjet optimization

Fig. 14 shows the convergence of the particles to the minimum value of the objective function. The initial modified waterjet inlets that were used for the morphing showed a ~1% decrease in resistance compared to the original. The optimized waterjet inlet shows a 2.3% reduction in resistance.



**Fig. 14.** Convergence of objective function for JHSS waterjet optimization, particles colored with objective function values

#### 4.3 DC barehull optimization

The DC barehull optimization utilized five design variables. The topology map is not shown since it is difficult to visualize a 5-dimensional topology map. An eighteen particle swarm approach was used. Fig. 15 shows the convergence of the swarm for the 5 design variables, and Fig. 16 shows the convergence of the swarm to the minimal objective function.

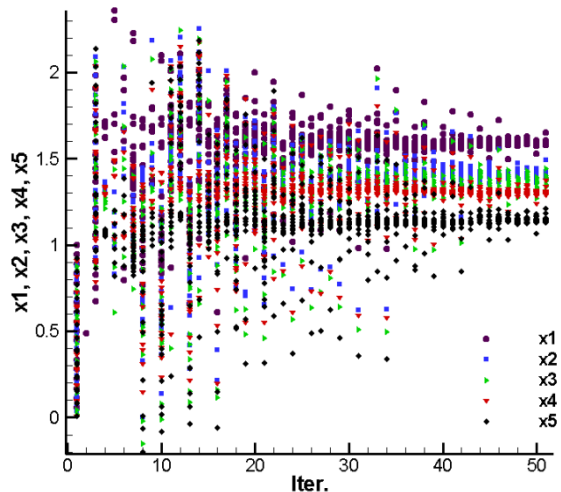


**Fig. 15.** Convergence of design variables for DC barehull optimization

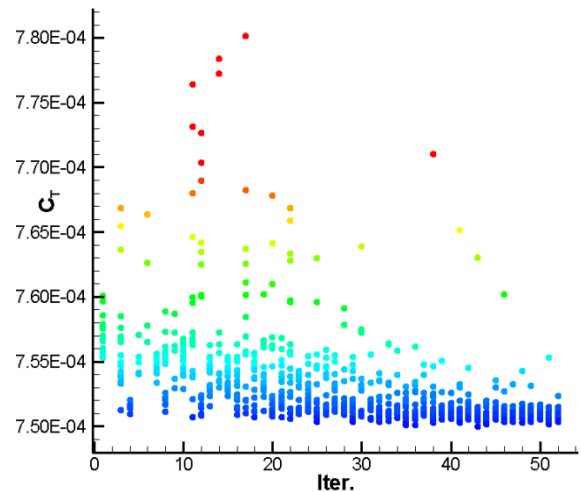


**Fig. 16.** Convergence of objective function for DC barehull optimization, particles colored with objective function

The final optimized hull form shows a 3% decrease in resistance compared to the original. Tahara *et al.* (2011) used just three of the six geometries used here for morphing, for their multi-objective GA optimization and obtained a reduction of ~4%, indicating that the PSO for the DC may have converged at a local minima too.

#### 4.4 DC waterjet inlet optimization

The original waterjet will be appended to the best optimized DC barehull grid after thorough inspection of both the PSO optimized and GA optimized geometries. A few modifications to the inlet will be made to have it flush with the optimized hull. Based on the previous sensitivity studies, a new sensitivity study will be carried on the hull shape. Since the inflow to the waterjet will be altered due to the hull form modification, the previous sensitivity study on the waterjet appended to the original hull may no longer be valid. Work is in progress and results will be included in the final paper.

### 5.0 CONCLUSIONS

Simulation based design optimization is performed on two waterjet appended ships, the JHSS and the Delft catamaran. There is a strong coupling between the Delft catamaran hull shape and the inlet capture area for the waterjet. A variable physics SBD method has been employed for the Delft catamaran in which the initial optimization of the bare hull is conducted with the integral force/moment CFD waterjet model, and then the selected optimized barehull is appended with the waterjet and the waterjet inlet is optimized. The bow shape optimization and waterjet inlet optimization of the JHSS were done independent of each other since the bow shape modification does not affect the local flow near the waterjet inlet. Also, the CFD waterjet model was not used for JHSS since the waterjet induced forces and moments had negligible effect on the sinkage and trim of the hull.

The particle swarm optimizer is used for the optimization. The high performance computing URANS code, CFDShip-Iowa is used for the flow solver. A morphing type geometry modification scheme is used where the initial geometries define the design search space. The initial geometries are obtained through geometry modification sensitivity studies to find a feasible search space.

The overall optimization methodology gave 6.7% resistance reduction for JHSS bow shape, 2.3% resistance reduction for JHSS waterjet inlet, and 3% resistance reduction for the DC barehull (with waterjet model). Work for the Delft catamaran waterjet inlet optimization is in progress and will be included in the final paper. The effect of combining the adjacent inlets of the JHSS waterjets was also studied, and it showed a 7% decrease in overall resistance warranting further studies.

Comparison with concurrent and complementary multi-objective optimization results of the bare hull JHSS and Delft catamaran (Tahara *et al.*, 2011) revealed that at current settings, the PSO tends to get stuck in local minima, whereas GA does not. This issue needs to be addressed by re-running the PSO JHSS bow form optimization with more number of swarm particles and fine tuning the cognitive, social, random and inertia parameters to find the best parameters.

## REFERENCES

- Campana, E.F., Peri, D., Tahara, Y., & Stern, F. (2006) "Shape Optimization in Ship Hydrodynamics using Computational Fluid Dynamics." *Computer Methods in Applied Mechanics and Engineering*, 196, pp. **634–651**.
- Campana, E.F., Peri, D., Tahara, Y., Kandasamy, M., & Stern, F. (2009) "Numerical Optimization Methods for ship Hydrodynamic Design," *Trans. SNAME Annual Meeting*, Providence, Rhode Island, USA.
- Carrica, P., Huang, J., Noack, R., Kaushik, D., Smith, B., and Stern, F. (2010). "Large-Scale DES Computations of the Forward Speed Diffraction and Pitch and heave Problems for a Surface Combatant." *Computers & Fluids* **39** (7), pp. 1095-1111
- Kandasamy, M., Ooi, S.K., Carrica, P., & Stern, F. (2010) 'Integral force/moment water-jet model for CFD simulations', *Journal of Fluids Engineering*, Vol. 132, 101103-1
- Kandasamy, M., Georgiev, S., Milanov, E., Stern, F. (2011) 'Numerical and experimental evaluation of waterjet propelled Delft catamarans.' *submitted to FAST 2011*, Hawaii
- Kandasamy, M., Ooi, S.K., Carrica, P., Stern, F., Campana, E., Peri, D., Osborne, P., Cote, J., Macdonald, N., & de Waal, N. (2009) "URANS based optimization of a high speed foil assisted semi planning catamaran for low wake." *Proc. 10th International Conference Fast Sea Transportation*, Athens, Greece.
- Peri, D., Campana, EF., Tahara, Y., Kandasamy, M. & Stern, F. (2010) "New developments in Simulation-Based Design with application to High Speed Waterjet Ship Design." *Proc. 28th Symposium on Naval Hydrodynamics*, Pasadena, USA.
- Tahara, Y., Hino, T., Kandasamy, M., He, W., Stern, F. (2011) "CFD-based multiobjective optimization of waterjet propelled high speed ships." *submitted to FAST 2011*, Hawaii
- Tahara, Y., Peri, D., Campana, EF. & Stern, F. (2008a) "Computational fluid dynamics-Based multiobjective optimization of a surface combatant." *J. Marine Science and Technology*, 13(2), pp. 95-116.
- Tahara, Y., Peri, D., Campana, EF., & Stern, F. (2008b) "Single and Multiobjective Design Optimization of a Fast Multihull Ship: numerical and experimental results." *Proc. 27th Symposium on Naval Hydrodynamics*, Seoul, Korea.
- Takai, T. (2010). 'Simulation based design for high speed sea lift with waterjets by high fidelity URANS approach.' *Master's Thesis, The University of Iowa*.
- Takai, T., Kandasamy, M., & Stern, F., (2011). 'Verification and validation study of URANS simulations for axial waterjet propelled large high speed ship', *submitted to Journal of Marine Science and Technology*.

## ACKNOWLEDGEMENTS

This work is sponsored by the US Office of Naval Research through research grants N00014-08-0491, under the administration of Dr. Ki-Han Kim. The simulations were performed on 4.7GHz IBM Power 6 machine '*DaVinci*' at the DoD NAVO center.